Towards first-principles prediction of polymer configurational statistics*

A. R. Tiller
Biosym Technologies Ltd, Unit 17, Intec 2, Wade Road, Basingstoke, RG24 8NE, UK

Conformational energy calculations are used to develop a rotational isomeric state (RIS) model for polystyrene including t, g and $\bar{g}$ states. No adjustment is made to match experimental data as with an earlier two-state model due to Yoon and coworkers. The three-state model correctly predicts a higher limiting characteristic ratio for the syndiotactic polymer as compared to the isotactic. It is shown how molecular dynamics simulations on a periodic cell containing polystyrene fragments in a Θ solvent can be used to make a systematic correction for the short-range solvent effect, enhancing the tendency of the syndiotactic chain to expand relative to the isotactic chain. After solvent correction, C_∞ is predicted about 26–28% too low for both isotactic and syndiotactic polystyrene, a deviation that can be attributed to other approximations inherent in the RIS method.

(Keywords: RIS theory; polystyrene; molecular dynamics)

INTRODUCTION

Rotational isomeric state (RIS) theory is a long-established approach to understanding the configurational statistics of chain molecules[1]. Such an understanding is important because many macroscopic properties of polymers are influenced by the distributions in size and shape of the individual polymer chains. RIS theory, sometimes combined with Monte Carlo methods[2], enables these size and shape distributions to be characterized. Averages and distributions of quantities such as the end-to-end distance, radius of gyration and persistence vector can be correlated with a range of important, experimentally measurable properties, including viscosity[3], entanglement molecular weight[4], plateau modulus[5], macrocyclization equilibria[6] and the tendency to form liquid-crystalline phases[7].

The RIS method makes two important approximations. First, fixed bond lengths and valence angles are assumed, so that the polymer conformation is considered to depend significantly only on the values of the dihedral angles about bonds in the chain backbone. Secondly, instead of being allowed to vary continuously between 0 and 360°, backbone dihedral angles are restricted to certain discrete values, *trans* (t) and *gauche* (g, $\bar{g}$) states being typical for vinyl chains. Owing to steric considerations (the 'pentane effect'), the values of these backbone dihedral angles cannot be considered independently of the values of neighbouring dihedral angles; a g state in polyethylene, for example, is far more likely to neighbour a t state than a $\bar{g}$ state. However, it is commonly assumed that the rotational potential affecting any given backbone bond, i, depends only on the dihedral angles of the immediate neighbours, $i-1$ and $i+1$, interactions of longer range being unimportant.

RIS theory requires a statistical weight matrix for each 'bond pair' (a pair of neighbouring dihedral angles) in the polymer backbone. These statistical weight matrices can be estimated by calculating the relative energies of different conformations of a molecular fragment containing the bond pair of interest[1,8,9]. In early work on polystyrene[9], different conformations of the *racemic* and *meso* dyads of the fragment CH_3–$CH(C_6H_5)$–CH_2–$CH(C_6H_5)$–CH_3 were generated by varying the two central dihedral angles. Contour maps of relative energy as a function of these two angles were obtained using torsional and non-bond potential-energy functions, and statistical weights estimated by careful analysis of the conformational domains surrounding the minima. At the time this work was carried out, further approximations were necessary in order to make the calculations tractable. For example, the bond lengths and valence angles were treated as fixed for the purpose of evaluating the energy, with the same values being assigned to all conformations. Furthermore, the phenyl substituent was confined to orientations in which its plane is perpendicular to the plane defined by the backbone bonds neighbouring the carbon atom to which it is attached.

Advances in computer hardware and software enable these types of calculation to be performed much more rapidly today. Furthermore, the additional approximations required to make the original calculations tractable are no longer necessary. Procedures for estimating statistical weight matrices have been automated using force-field-based molecular mechanics methods[2], and RIS calculations using such *ab initio* statistical weights can predict trends in the chain shape characteristics amongst polymers with similar chemical structure.

* Presented at 'The Polymer Conference', 20–22 July 1993, University of Cambridge, UK

0032-3861/94/21/4511-10

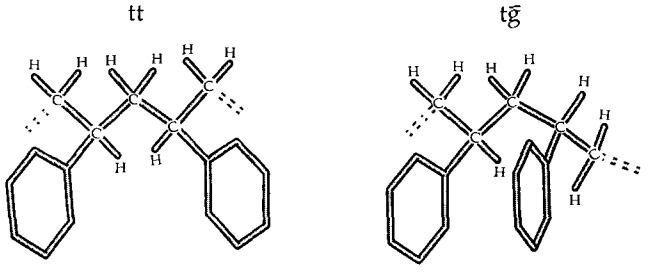

Figure 1 The *tt* and *tḡ* conformational states of a *racemic* dyad in polystyrene, illustrating the different potential for interaction between the phenyl substituents and surrounding solvent molecules

However, quantitative prediction of measurable properties such as the characteristic ratio is more difficult. Statistical weights that are capable of reproducing quantitative results have generally been obtained by adjusting the *ab initio* statistical weights to fit experimental data[9]. For the design of new polymers, it is desirable to predict properties without first having to carry out synthesis and characterization, and it is therefore desirable that statistical weight matrices capable of reasonable quantitative predictions should be obtained from first principles.

One potential problem with the *ab initio* estimation of statistical weights described above is that the energy calculations are carried out on the molecular fragments in vacuum. In real systems, the presence of surrounding solvent molecules may act to lower the energy of conformations disfavoured in the vacuum.

For example, consider the *racemic* dyad $-CH_2-CH(C_6H_5)-CH_2-CH(C_6H_5)-CH_2-$ shown in *Figure 1*. In the *tḡ* state, the phenyl substituents are close enough to interact strongly with each other. However, in the *tt* state, the pheyl substituents extend outward into the surrounding solvent. It is likely that the energy of the *tt* stage will be estimated too high relative to the *tḡ* state in the vacuum calculations because there are no solvent molecules present to compensate for the absence of phenyl–phenyl interactions.

Yoon *et al.* compensated for this short-range solvent effect by truncating the non-bond interaction potential in their calculations on polystyrene[9]. There is, however, no general prescription for applying corrections of this type. Neither is the importance of this solvent effect known relative to other approximations used to obtain the statistical weights, such as the quality of the force field employed to calculate the conformational energies. This work aims to determine the influence of the short-range solvent effect upon the statistical weight matrices for polystyrene.

CONFORMATIONAL ENERGIES OF POLYSTYRENE FRAGMENTS

In order to obtain statistical weights, the total conformational energy of a polymer consisting of n backbone bonds is divided into $n-2$ energy terms, each dependent upon a pair of consecutive backbone rotation angles (p. 62 of ref. 1). The term depending upon the rotation angles (ϕ_i, ϕ_{i+1}) of bonds i and $i+1$ is defined to include 'first-order' non-bond interaction energies, which depend exclusively upon ϕ_{i+1}, and 'second-order' interactions, which depend jointly upon ϕ_i and ϕ_{i+1}. Third- and higher-order non-bond interactions (i.e. those which depend upon three or more backbone rotation angles) are not counted.

Conformational energies of three fragments, each containing four backbone bonds from a polystyrene chain, were calculated using molecular mechanics methods[10]. The fragments modelled were the *racemic* and *meso* dyads of $C-CH(C_6H_5)-CH_2-CH(C_6H_5)-C$, and the fragment $C-CH_2-CH(C_6H_5)-CH_2-C$. These fragments are shown in *Figure 2*, and are hereafter referred to as A, B and C respectively. In contrast with the original work of Yoon *et al.*[9], carbon atoms at each end of the fragments are stripped of all pendent atoms and groups. This ensures that third-order interactions are not included in the conformational energy, in accordance with the definition of statistical weights that we use (p. 62 of ref. 1). Alternative fragments A′, B′ and C′ (corresponding to the fragments studied in the original work) are also considered below. Here, the naked carbon atoms terminating fragments A, B and C are replaced by methyl groups.

Conformations were generated by rotating the dihedral angles about each of the two central backbone bonds (ϕ_i and ϕ_{i+1}) through 360° in 10° steps (see *Figure 2*). The geometry of the fragment was then optimized by molecular mechanics techniques[11] in each of the resulting 1296 conformations, with the dehedral angles about the two central bonds fixed at the chosen values.

Two methods of geometry optimization were used. In the first method, referred to hereafter as 'constrained optimization', all bond lengths and bond angles were fixed, and the plane of the phenyl substituents was constrained to lie perpendicular to the polymer backbone. The constrained optimization therefore corresponds to the approximations made in the original work[9]. In the second method, referred to hereafter as 'free optimization', all internal degrees of freedom (except for the two fixed dihedral angles) were allowed to vary. Following the original work[9], Coulombic interactions were ignored, so that only van der Waals interactions were included in the non-bond energy. The energy calculations were carried out using a modified version of the pcff91 force field[11]*.

CONSTRAINED OPTIMIZATION

Figure 3 shows conformational energy maps for fragments A and B that result from the constrained method of geometry optimization. For the *racemic* dyad (A), the

* The pcff91 force field does not contain an explicit term describing the intrinsic torsional potential for c–c–c–cp (where c denotes the potential type for carbon atoms in the chain backbone, and cp for carbon atoms in the phenyl substituent). In this work, the above term is set equal to the corresponding term for c–c–c–c

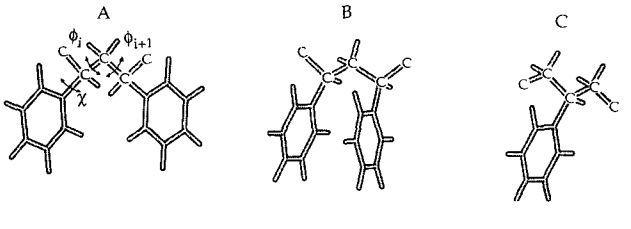

Figure 2 Four-bond fragments, A (*racemic* dyad), B (*meso* dyad) and C, used for conformational energy calculations

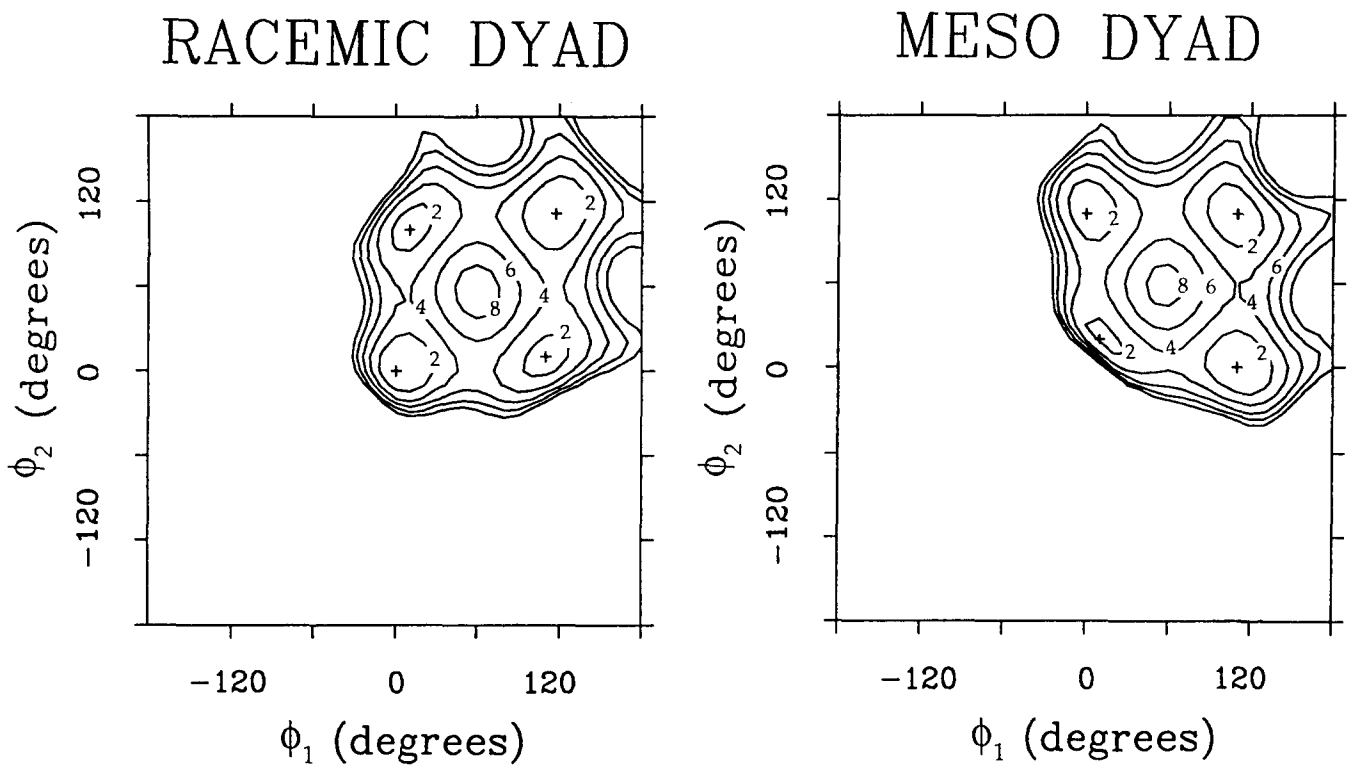

Figure 3 Conformational energy maps for the *racemic* and *meso* dyads (fragments A and B respectively) obtained from the method of constrained optimization. Conventions for measuring angles are given in the text. Contours are plotted at intervals of 2 kcal mol^{-1}, and local energy minima are marked with a + symbol

torsional angles ϕ_i and ϕ_{i+1} are measured in the right-handed sense for the *dd* enantiomorph, and in a left-handed sense for the *ll* enantiomorph. (Note that this notation refers to the chirality of the *bonds* i and $i+1$, so that the *ll* enantiomorph has an *l* centre at the first α carbon, and a *d* centre at the second.) The *trans* state corresponds to a dihedral angle of 0°. For the *dl* meso dyad (B), ϕ_i and ϕ_{i+1} are measured in right- and left-handed senses respectively, with a corresponding reversal for the *ld* dyad. Energy values are given relative to the energy minimum of the racemic *tt* state. These are the same conventions as used in the original work[9].

As expected, the conformational energy map for the *racemic* dyad is very similar to that of Figure 4 in ref. 9. Note especially the high energies of the $\bar{g}$ conformations (ϕ_1 or $\phi_2 \sim -120°$), in which severe steric overlaps occur. The *tt* state has the lowest energy, followed by the *gg* state at $+0.155$ kcal mol^{-1}, and the $\{tg\}$ states at $+1.029$ kcal mol^{-1}; the curly brackets denote the set of symmetry-related states, *tg* and *gt* in this case. The $\{g\bar{g}\}$ states appear at around $+7$ kcal mol^{-1}. The energies of the *gg* and $\{tg\}$ states are closer to the *tt* state than in the original work, which can be attributed to differences in the force field used and to termination of the fragment with naked carbon atoms in the present work.

The conformational energy map for the *meso* dyad shows a very slight asymmetry (an artefact of the molecular mechanics calculations) but is qualitatively similar to that of Figure 3 in ref. 9. Again the $\bar{g}$ conformations have very high energies. However, there are some differences compared to the original work, which are attributable to the force field and to the method of terminating the fragment. For example, a single rather than a double minimum for the *gg* state is found in the present work. The relative ordering of the *tt*, $\{tg\}$ and *gg* states ($+1.60$, $+0.365$ and $+0.571$ kcal mol^{-1} respectively) is also different from ref. 9.

FREE OPTIMIZATION

Figure 4 shows conformational energy maps for fragments A and B that result from the free optimization calculations. It is immediately obvious that these maps differ qualitatively from those obtained using constrained geometry optimization. In particular, the energies of the $\bar{g}$ conformations are considerably lowered in both the *racemic* and *meso* dyads, an effect directly attributable to allowing rotation about the bond connecting the phenyl substituent to the chain backbone (see *Figure 5*). Yoon *et al.* anticipated this effect, of course[9], but estimated that, even allowing for such rotation, the energies of the $\bar{g}$ conformations would be so high that the $\bar{g}$ states could be ignored. The results of the free optimization study suggest that this is not the case, and that a three-state rotational isomeric state scheme should be developed for polystyrene to take account of *t*, *g* and $\bar{g}$ states. The statistical weights derived below are therefore in the form of 3×3 matrices, rather than the 2×2 matrices previously obtained from the two-state (*t*, *g* only) model.

Figure 5 plots dihedral angles (χ) about the bonds connecting phenyl substituents to the backbone for each of the minimum energy states of the *racemic* dyad. Angle $\chi = 90°$ corresponds to the case where the phenyl ring is perpendicular to the plane defined by the backbone atoms (as in the constrained optimization). Both phenyl substituents lie close to $\chi = 90°$ in the *tt*, *gg* and $\{tg\}$ states. However, in the $\{t\bar{g}\}$ and $\{g\bar{g}\}$ states one of the

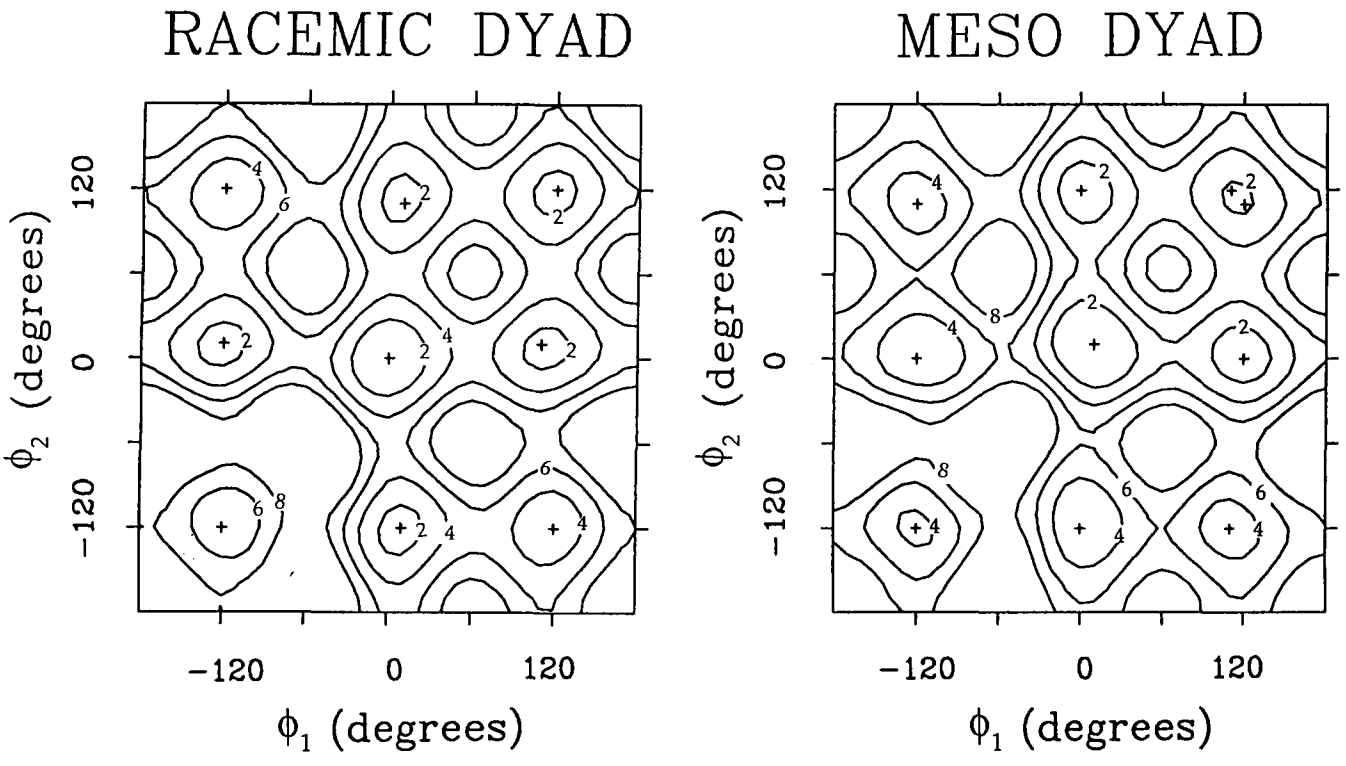

Figure 4 Conformational energy maps for the *racemic* and *meso* dyads obtained from the method of free optimization. Contours are plotted at intervals of 2 kcal mol^{-1}, and local energy minima are marked with a + symbol

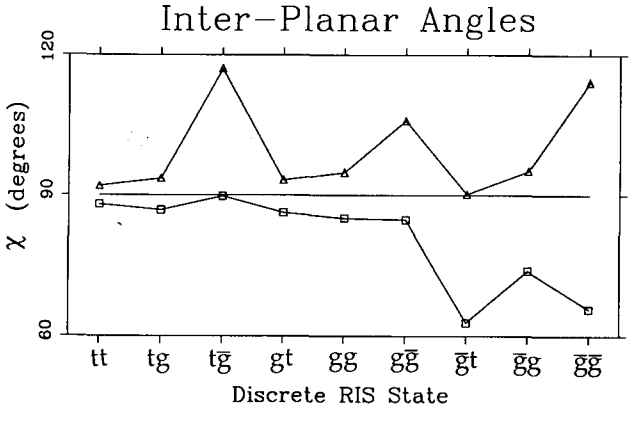

Figure 5 Angle adopted in the minimum energy conformations of the *racemic* dyad between the plane of each phenyl substituent and the plane defined by the neighbouring polymer backbone atoms. Angle $\chi = 90°$ indicates that the phenyl substituent is perpendicular to the backbone

two χ angles in the fragment deviates significantly (by as much as 30°) from the perpendicular geometry, and in the $\bar{g}\bar{g}$ state both χ angles deviate. The *meso* dyad exhibits similar behaviour.

The following energies (kcal mol^{-1}) are calculated for the *racemic* dyad: *tt*, 0.0; $\{t\bar{g}\}$, 1.143; *gg*, 1.346; $\{tg\}$, 1.382; $\{g\bar{g}\}$, 2.501; and $\bar{g}\bar{g}$, 4.470. Notice that the $\{t\bar{g}\}$ states have the lowest energy after the *tt* state. The *gg* and $\{tg\}$ states have lower energies relative to *tt* than in the original work.

The following energies (kcal mol^{-1}) are calculated for the *meso* dyad: *tt*, −0.664; $\{tg\}$, 0.853; *gg*, 1.712; $\{t\bar{g}\}$, 2.070; $\{g\bar{g}\}$, 2.953; and $\bar{g}\bar{g}$, 3.515. It is interesting to note that the double minimum of the original work for the *gg* state is found by the free optimization calculations. However, there are some differences compared to ref. 9; for example, the *gg* and $\{tg\}$ states have lower energies relative to *tt*, and the energy of the *meso tt* state is found to be lower than that of the *racemic tt* state.

CALCULATION OF STATISTICAL WEIGHT MATRICES

The statistical weight matrix (u_{jk}) for a bond pair (ϕ_i, ϕ_{i+1}) is given in the following form:

$$u_{jk} = A_{jk} \exp[-(\varepsilon_{jk}/RT)]$$

where j denotes the rotational state of the first bond (ϕ_i) and k denotes that of the second bond (ϕ_{i+1}). The pre-exponential factor is used to account for differences in the shapes of potential-energy wells corresponding to the various rotational states of the bond pair.

In order to determine the discrete states to be used in the RIS representation of a bond pair, the contour map of energy, $E^t(\phi_i, \phi_{i+1})$, as a function of the two torsion angles is divided into a set of regions (see *Figure 6*). Normally, each local minimum is assigned to a distinct region. However, in cases where two local minima are very close (such as the double minimum in the *gg* state of the *meso* dyad) they can be grouped together into a single region, which then allows the representation of both minima as a single state on the map.

The energy values, $E^t(\phi_i, \phi_{i+1})$, include all first-order and second-order interactions in the fragment; first-order interactions depend on exactly one torsion angle, and second-order interactions depend on exactly two. According to our definition, the statistical weight matrix for a given bond pair should account for all second-order interactions in the fragment, but only those first-order interactions which depend on the second torsion angle, ϕ_{i+1}. In order to obtain the statistical weights from the

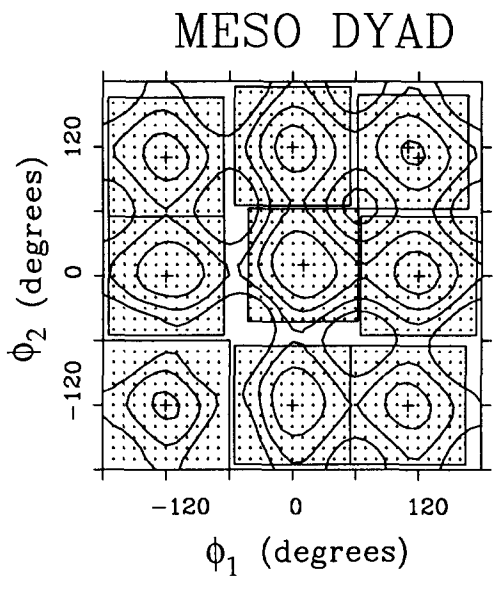

Figure 6 Conformational energy map for the *meso* dyad divided into nine regions. The average conformation at 300 K in each region corresponds to a discrete RIS state

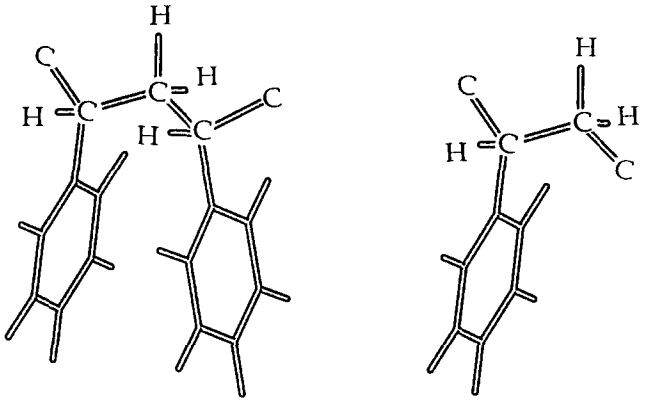

Figure 7 The *meso* dyad (fragment B) and the sub-fragment taken from it in order to calculate $E^{seg}(\phi_i)$

energy map, the energy, $E^{seg}(\phi_i)$, due to the first-order interactions dependent on ϕ_i is subtracted from $E^t(\phi_i, \phi_{i+1})$, and the resulting energies are denoted $E^{net}(\phi_i, \phi_{i+1})$. Additional molecular mechanics calculations were performed on an appropriate segment taken from each of the fragments, A, B and C, in order to determine $E^{seg}(\phi_i)$. *Figure 7* shows the segment used for the evaluation of $E^{seg}(\phi_i)$ for the *meso* dyad. Once this has been done, $E^{net}(\phi_i, \phi_{i+1})$ is calculated as:

$$E^{net}(\phi_i, \phi_{i+1}) = E^t(\phi_i, \phi_{i+1}) - E^{seg}(\phi_i)$$

The partition function, z_r, for each region r is then calculated at a given temperature (300 K for the polystyrene fragments in this study) using $E^{net}(\phi_i, \phi_{i+1})$. Statistical weights for each region can then be obtained from the formula:

$$u_{jk} \equiv u_r = z_r / z_{ref}$$

where z_{ref} is the partition function for a reference region, which is chosen to be that with the minimum average value of $E^{net}(\phi_i, \phi_{i+1})$.

The locations of the discrete states, or (ϕ_i, ϕ_{i+1}) pairs, to be used in the RIS approximation are obtained from the average values of the two torsional angles in each region of the $E^t(\phi_i, \phi_{i+1})$ map. However, if two or more regions have similar average ϕ_i (or ϕ_{i+1}) values, the number of discrete RIS states can be reduced by assigning a combined average value for the torsion angle to both regions. In this way, each bond in the pair is assigned to one of t, g, or $\bar{g}$ conformations, even though the actual value of the torsion angle corresponding to the t, g, or $\bar{g}$ conformation depends slightly upon the value of the neighbouring torsion angle. Further details can be found in refs. 2 and 9.

STATISTICAL WEIGHTS FROM THE FREE OPTIMIZATION

Table 1 shows the average angles $(\langle\phi_i\rangle, \langle\phi_{i+1}\rangle)$ in each of the discrete RIS states of fragments A, B and C. Symmetry requires that, according to our conventions for measuring the torsion angles, $\langle\phi_i\rangle$ and $\langle\phi_{i+1}\rangle$ should be identical for corresponding states. This is found to be the case (see *Figure 4* and *Table 1*) even though no symmetry constraints were imposed in the molecular mechanics calculations. For self-consistency, the discrete values of ϕ_{i+1} for a bond pair $(i, i+1)$ should be equal to the corresponding values of ϕ_{i+1} for the next bond pair along the polymer chain, $(i+1, i+2)$. The values in *Table 1* satisfy this condition to within less than 5° for any tacticity of the polystyrene chain.

RIS theory also requires fixed bond lengths and bond angles to be specified for the backbone bonds in the polymer chain. However, in the free optimization method the bond lengths and angles can vary slightly from one discrete RIS state to another. In the RIS calculations presented below, all C–C bond lengths in the polystyrene backbone were taken to be 1.53 Å. The statistical weight matrix for the bond pair $(i-1, i)$ is associated with the supplement to the bond angle between bonds i and $i+1$. We therefore assign a value to the bond angle between bonds i and $i+1$ given by the Boltzmann weighted average at 300 K of this bond angle at the conformational energy minima in the $E^t(\phi_{i-1}, \phi_i)$ map.

Statistical weight matrices obtained from the free optimization using the procedure outlined above are given in the Appendix, along with associated bond angle supplements. This three-state *ab initio* RIS scheme is referred to hereafter as model 1.

A second RIS model (model 2) was developed in the manner outlined above, but using fragments A′, B′ and C′ in the conformational energy calculations instead of A, B and C. These fragments are terminated by methyl groups, as in the original work of Yoon *et al.*, rather than with naked carbon atoms. Free optimization calculations again reveal the necessity to include $\bar{g}$ states, leading to a three-state RIS model.

Table 1 Averaged conformations of the discrete RIS states of fragments A, B and C at 300 K from the free optimization calculations

	$\langle\phi_i\rangle$ (deg)			$\langle\phi_{i+1}\rangle$ (deg)		
Fragment	$\bar{g}$	t	g	$\bar{g}$	t	g
A	−121.2	1.5	115.7	−121.2	1.5	115.7
B	−117.3	8.8	117.0	−117.3	8.8	117.0
C	−122.0	4.1	116.8	−122.0	4.1	116.8

Table 2 Summary of characteristic ratio results

	Isotactic C_∞(300 K)	Syndiotactic C_∞(300 K)	Atactic ($w_m=0.3$)[a] C_{200}(300 K)	Atactic ($w_m=0.5$) C_{200}(300 K)
Experiment	$\simeq 11$	–	$\simeq 10$ ($0.5 > w_m > 0.3$)	
Two-state model[9]	11.1	18.0	10.3	8.6
Model 1	9.8 (8.2[b])	10.7 (13.0[b])	12.5 (12.8[b])	13.9 (12.5[b])
Model 2	8.7	21.2	–	–

[a] Expectation of *meso* dyads $= w_m$
[b] Molecular dynamics solvent corrections applied

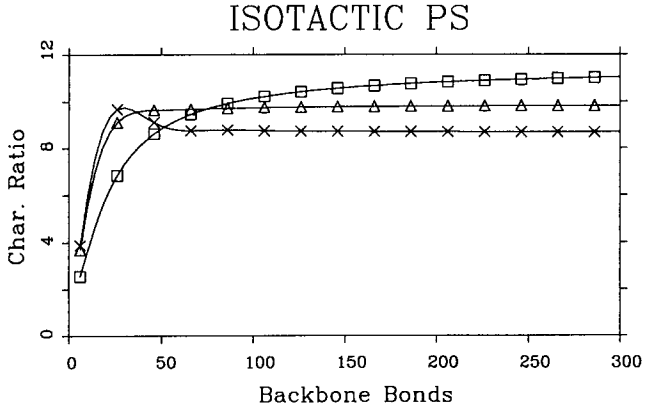

Figure 8 Characteristic ratio as a function of the number of backbone bonds for isotactic polystyrene at 300 K predicted by three RIS models: (□) two-state model of ref. 9; (△) model 1; (×) model 2

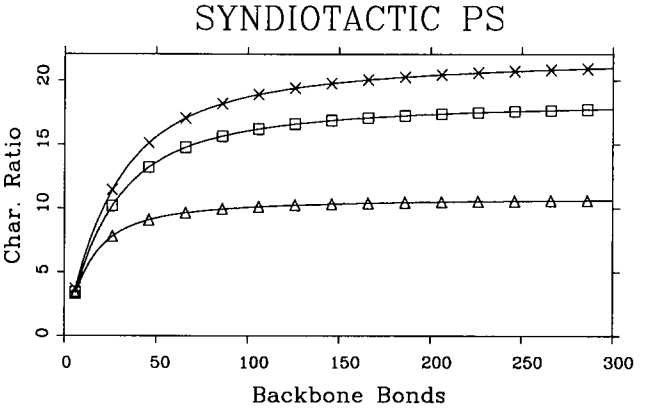

Figure 9 Characteristic ratio as a function of the number of backbone bonds for syndiotactic polystyrene at 300 K predicted by three RIS models: (□) two-state model of ref. 9; (△) model 1; (×) model 2

CHARACTERISTIC RATIOS

Predicted characteristic ratios of an n-mer chain, C_n, are chosen as a basis for testing the quality of the RIS model. This is done, firstly, because the characteristic ratio appears to be more sensitively dependent upon the statistical weight matrices than other properties, such as radius of gyration, and, secondly, because its limiting value (C_∞) can be correlated with several interesting properties, including entanglement molecular weight[4] and plateau modulus[5]. The characteristic ratio results are summarized in *Table 2*.

Figure 8 shows predicted characteristic ratios for isotactic polystyrene as a function of chain length at 300 K for three RIS models. For each of these models, the characteristic ratio has almost reached its limiting value when the chain contains 300 backbone bonds (i.e. a 150-mer). The curve marked with squares results from using the two-state model developed in the original work of Yoon *et al.*, in which the statistical weights were modified to achieve agreement with experimental data[12,13]. A limiting characteristic ratio of 11.1 is obtained, in good agreement with experimental values[12–14]. The curve marked with triangles gives the results of model 1 developed using the free optimization method in this work. The characteristic ratio reaches its limiting value more rapidly in this scheme, and C_∞ is slightly underestimated at 9.8. The curve marked with crosses represents the results of model 2, developed from conformational energy calculations on the A′, B′ and C′ fragments, and the limiting characteristic ratio of 8.7 is again too low.

Figure 9 shows the results of calculations on syndiotactic polystyrene. The three models all agree that the syndiotactic chain should have a higher limiting characteristic ratio than the isotactic, but the *ab initio* values for C_∞ differ significantly from the result of the two-state model. Although in this case there are no experimental data available for direct comparison, it seems reasonable to assume that the two-state model, derived by fitting to experimental data for the isotactic and atactic chains, should provide reasonably accurate values. The two *ab initio* curves straddle the two-state model results; the limiting characteristic ratios are 18.0, 10.7 and 21.2 for the two-state scheme, model 1 and model 2 respectively. One effect of terminating the fragments A′, B′ and C′ with methyl groups is that the g and $\bar{g}$ states have lower probability relative to t in model 2 on account of unfavourable third-order interactions between the terminal hydrogen atoms. This has a particularly noticeable influence on the statistical weight matrix of fragment A′ (the *racemic* dyad), causing C_∞ to be considerably increased for the syndiotactic chain relative to model 1.

The results of model 2 are in slightly better overall agreement with the two-state model than those of model 1 for the isotactic and syndiotactic chains. This might tempt us to favour model 2 as a procedure for generating an RIS scheme. However, we are concerned with developing a consistent *ab initio* method for deriving statistical weight matrices, ultimately corrected to account for short-range solvent effects. As such, we choose to continue with model 1 for consistency with our definition of statistical weights.

Figure 10 shows the temperature dependence of C_{200} (a very good approximation to C_∞) for two ensembles of atactic polystyrene chains. Each ensemble consists of 20 atactic 200-mer chains. In the first, the expectation (w_m)

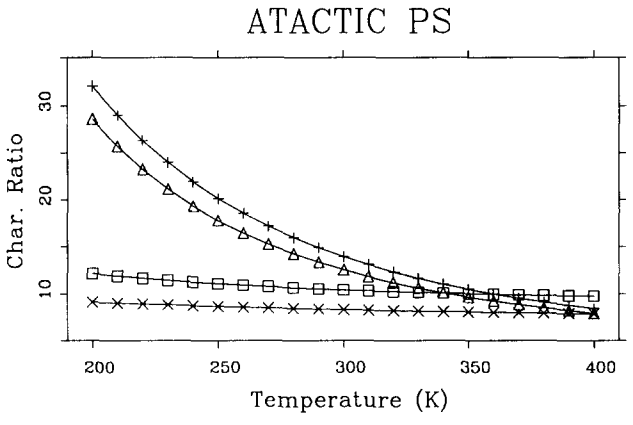

Figure 10 Temperature dependence of C_{200} for two ensembles of atactic polystyrene chains: (□) two-state model of ref. 9, $w_m=0.3$; (× two-state model of ref. 9, $w_m=0.5$; (△) model 1, $w_m=0.3$; (+) model 1, $w_m=0.5$

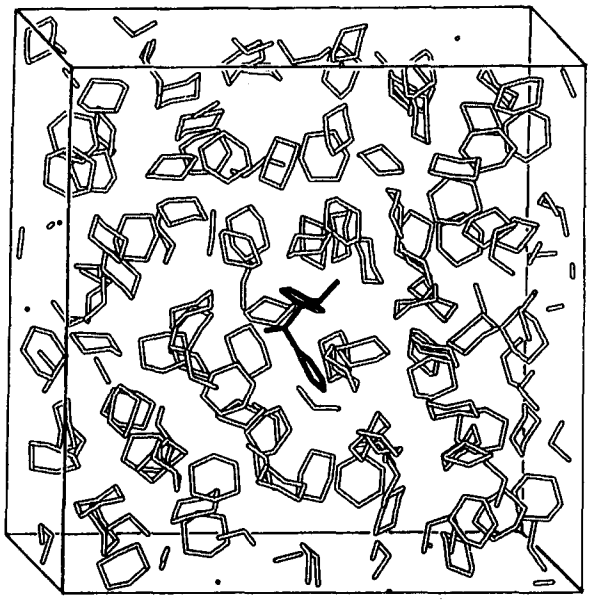

Figure 11 Model periodic simulation cell containing fragment A′ ($t\bar{g}$ conformation) in a Θ solution of cyclohexane

of *meso* dyads is 0.3, and in the second $w_m=0.5$. Such ensembles were also considered in the original work[9] as limiting cases between which conventional atactic polystyrenes are believed to lie[15]. At low temperatures, characteristic ratios from model 1 are higher than those of the two-state scheme, although the results become very similar above 350 K. Both models predict a negative temperature coefficient in agreement with experimental observations[16]. Model 1 makes the opposite prediction to the two-state scheme that C_{200} is higher for the case $w_m=0.5$ than for $w_m=0.3$ at all temperatures.

SOLVENT CORRECTION

As already mentioned, the vacuum conformational energy maps should be corrected to take account of the short-range solvent effect. We first assign each conformation of a fragment to either *open*, if the phenyl substituents extend out into the vacuum, or *closed*, if the phenyl substituents interact strongly with each other. For example, the *tt* conformation of the *racemic* dyad is an *open* state, whereas the $t\bar{g}$ conformation is *closed* (see *Figure 1*). The full list of states considered to be *closed* is: *meso tt*; *meso* $\bar{g}\bar{g}$; *racemic* $\{t\bar{g}\}$. A crude perturbation correction to the conformational energy maps is made by lowering the energy of *open* states relative to *closed* states as described below.

Molecular dynamics simulations[17] of polystyrene fragments in a Θ solvent were carried out in order to estimate the difference in solvent stabilization between *open* and *closed* states. A periodic box containing 100 cyclohexane molecules was first constructed at the experimental density, and thoroughly equilibrated at 20°C using constant-volume molecular dynamics. Fragment A′, the *racemic* dyad terminated by methyl groups, was then randomly oriented and 'soaked' using this solvent box so as to create a periodic cell of side 30 Å (see *Figure 11*). Twelve such cells were constructed, six containing fragment A′ in the *tt* (*open*) conformation, and six in the $t\bar{g}$ (*closed*) conformation. Each cell was first equilibrated at 35°C (the Θ temperature of polystyrene in cyclohexane), and then simulated for 10 ps by constant-volume molecular dynamics using the modified pcff91 force field (see earlier footnote). The central dihedral angles in the fragment were constrained to maintain their *tt* or $t\bar{g}$ conformation throughout each simulation, but all other degrees of freedom were allowed to vary. The effect of Coulombic interactions, which were included in the calculations, was found to be very small (see below), providing some justification for their neglect in the vacuum conformational energy calculations on the fragments. A non-bond potential cut-off of 9 Å was used, and the total simulation time was of the order of 10 CPU hours for a single MD run on a Silicon Graphics R4000 Indigo workstation. During the final 10 ps of each simulation, the energy of interaction between the solvent molecules and the fragment was evaluated and stored every 100 fs. Thus each simulation provides 100 values of the fragment–solvent interaction energy, giving a total of 600 values for the *tt* conformation and 600 for the $t\bar{g}$ conformation. These values are plotted in *Figure 12*, and summarized in *Table 3*.

Figure 12 shows large fluctuations in the fragment–solvent interaction energy during the molecular dynamics

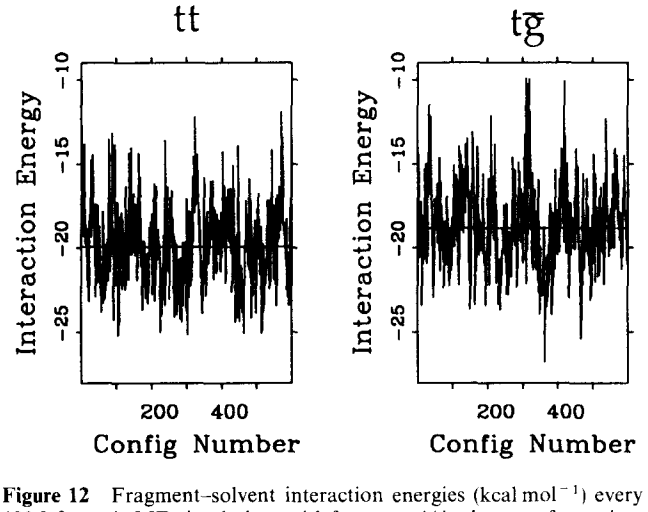

Figure 12 Fragment–solvent interaction energies (kcal mol^{-1}) every 100 fs from six MD simulations with fragment A′ in the *tt* conformation, and six simulations with fragment A′ in the $t\bar{g}$ conformation. Average values are plotted as horizontal lines on the graphs

Table 3 Average fragment–solvent interaction energies (kcal mol^{-1}) from MD simulations

	Run number[a]						
	1	2	3	4	5	6	Average[b]
tt	−19.5(0.3)	−20.0(0.2)	−20.8(0.2)	−19.3(0.2)	−20.1(0.3)	−19.7(0.2)	−19.9(0.1)
$t\bar{g}$	−18.7(0.2)	−18.2(0.3)	−19.2(0.2)	−19.5(0.3)	−19.0(0.3)	−18.3(0.2)	−18.7(0.1)

[a] Average (standard error on the mean) of 100 energies from a single MD run
[b] Average (standard error on the mean) of all 600 energies

Table 4 Connolly contact surface areas (Å^3) between a hydrogen atom probe and different conformations of the A′ and B′ fragments[a]

Conformation	*tt*	{*tg*}	{$t\bar{g}$}	*gg*	{$g\bar{g}$}	$\bar{g}\bar{g}$
A′	153.5 (o)	156.2(o)	139.7(c)	155.4(o)	161.0(o)	155.5(o)
B′	139.4(c)	157.3(o)	152.4(o)	161.0(o)	154.0(o)	137.7(c)

[a] (o) signifies an *open* state, (c) a *closed* state

simulations. However, the results in *Table 3* show that there is a statistically significant difference in the average interaction energy over the 600 data points between *tt* and $t\bar{g}$ conformations. As expected, the solvent has a greater stabilizing effect (more negative interaction energy) on the *open* (*tt*) conformation; on the basis of the MD simulations the magnitude of this effect is predicted to be a little over 1 kcal mol^{-1}. We take this value to be representative of solvent stabilization of all *open* states relative to *closed* states.

Average interaction energies for each of the six different simulations on a given conformation show variations greater than the standard error in any one of these averages (see *Table 3*). This indicates a slight dependence of the interaction energy upon starting conformation, although it is clear that this effect will not significantly change the overall result.

The fragment–solvent interaction energy can be divided into contributions from van der Waals and Coulombic terms. We find that the contribution of Coulombic terms to the average interaction energy is very small: −0.14 (±0.01) kcal mol^{-1} in the *tt* conformation, and −0.16 (±0.01) kcal mol^{-1} in the $t\bar{g}$ conformation. Furthermore, the magnitude of the Coulombic energy is never greater than 0.53 kcal mol^{-1} in any of the 1200 configurations saved from the molecular dynamics simulations. It is therefore clear that the difference in fragment–solvent interaction energy between *open* and *closed* states is due to van der Waals interactions.

It is interesting to compare our value of 1 kcal mol^{-1} solvent stabilization for *open* states with the effect of truncating the non-bond potential function for all atom pairs at 5.0 Å — a method of correcting for the solvent effect previously proposed[9]. For example, the energy of the *meso tg* (*open*) state decreases relative to *tt* (*closed*) by 1.1 kcal mol^{-1} in this scheme, in very good agreement with our predictions. However, the energy of the *racemic gg* state decreases by 0.9 kcal mol^{-1} relative to *tt* under truncation of the non-bond potential, even though no effect is predicted in our present scheme as both states are *open*.

It is possible that the assignment of states to either *open* or *closed* is too simplified. Since the fragment–solvent interaction energy is dominated by van der Waals terms, it might be correlated with the contact surface area between the fragment and the solvent. Calculated Connolly contact surface areas[18] between a hydrogen atom probe of radius 1.1 Å and fragments A′ and B′ in different conformations are given in *Table 4*. The results justify our broad division of states into *open* and *closed* categories, although a more exact treatment might allocate a variable degree of *openness* and solvent stabilization to the different states. Indeed, correlation with Connolly contact surface area (an extremely fast calculation) might provide an efficient means of doing this.

We have approximated the complex effect of solvent on the conformational energy maps of *Figure 4* by making a simple perturbation correction. The energies of all conformations falling within *open* regions were lowered in proportion to their difference in energy compared to the minimum point of the region. In this way, the edges of the *open* regions were kept at their previous energies, and the local minima were lowered by 1.0 kcal mol^{-1}. The effect is much like dropping a stone into a net, where the net corresponds to the conformational energy surface plotted as a function of the two dihedral angles, and the rim of the net corresponds to the edge of a region as shown in *Figure 6*. The *closed* regions were not altered.

Statistical weight matrices were obtained from the new conformational energy maps exactly as described above, giving a solvent-corrected version of model 1. RIS calculations using this model were then carried out to determine characteristic ratios for isotactic and syndiotactic polystyrene, and for the two ensembles of atactic chains.

The limiting values of the characteristic ratio that result are given in *Table 2*. Compared to model 1, C_∞ is decreased by 1.6 for the isotactic chain (taking it further away from the experimental value), and increased by 2.3 for the syndiotactic chain (moving it towards the 'experimental' value). The solvent-corrected results for the isotactic and syndiotactic chains cannot be said to agree any better or any worse with experiment than those of model 1. The difference in characteristic ratio between the isotactic and syndiotactic chains is, however, increased by the solvent correction, in better agreement with the two-state model, and we may conclude that short-range solvent effects enhance the intrinsic tendency of the syndiotactic chain to expand relative to the isotactic polymer. Furthermore, the solvent-corrected results are

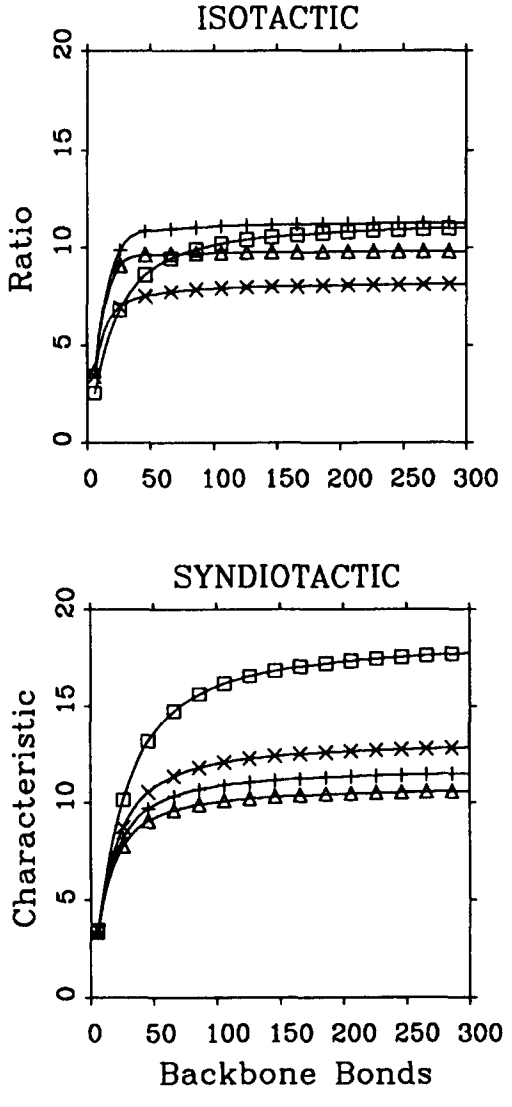

Figure 13 A comparison of the characteristic ratios predicted for isotactic and syndiotactic polystyrene from: (□) two-state model of ref. 9; (△) model 1; (×) solvent-corrected model 1; (+) model 1A (modified torsional potentials)

26% below the two-state model 'experimental' results for the isotactic chain, and 28% below for the syndiotactic chain, suggesting the possibility of a systematic error deriving from some other source. If this is indeed the case, the systematic error is masked without the solvent correction, in which case the errors are 12% and 41% respectively.

The solvent correction causes a slight increase in C_{200} for the $w_m=0.3$ atactic ensemble, and a slight decrease for the $w_m=0.5$ ensemble. C_{200} for the $w_m=0.3$ ensemble then becomes greater than that for the $w_m=0.5$ ensemble, in agreement with the prediction of the two-state model.

MAGNITUDE OF THE SOLVENT CORRECTION

We have seen that the solvent correction has a significant effect on the characteristic ratios predicted from model 1, in some respects providing insight in good accordance with experiment. However, it is instructive to consider the importance of the solvent effect relative to other factors, such as the quality of the forcefield employed in the conformational energy calculations. In order to test this, we have developed another RIS model (model 1A), in which the energy term describing the intrinsic torsional potential for rotation about C–C bonds is altered as described below.

In model 1, the forcefield term describing rotation about a C–C bond is:

$$E(\phi)=0.1223(1+\cos\phi)+0.0514(1+\cos 2\phi)$$
$$-0.2230(1+\cos 3\phi)$$

In model 1A, we somewhat arbitrarily increase the magnitude of the force constants by 20%, so that the new energy expression is:

$$E(\phi)=0.1467(1+\cos\phi)+0.0617(1+\cos 2\phi)$$
$$-0.2676(1+\cos 3\phi)$$

Figure 13 compares the characteristic ratios of isotactic and syndiotactic polystyrene from the two-state model, model 1, the solvent-corrected model 1 and model 1A. The changes to the torsional force constants in model 1A are seen to have an effect similar in magnitude to that of the solvent correction.

C_∞ for model 1A (+) is increased compared to model 1 (△) for both tacticities of the polystyrene chain, improving agreement with the two-state model; indeed, the result for the isotactic chan now matches experiment very well. It therefore seems conceivable that inaccuracies in the force field could introduce a systematic error into the predicted characteristic ratios, but it must be remembered that there are several other possible sources of error. For example, the results using model 2 above suggest that it is necessary to account for third- and higher-order interactions in the calculation of statistical weights, and furthermore the statistical weights should actually be determined from potentials of mean force rather than minimized energies. Neither have we accounted for the longer-range effect whereby monomers in a random coil are screened from interactions with the solvent by the presence of other monomers on the same chain. It is clear that further work is required in order to determine the influence of these approximations, and to find ways of correcting for them, before quantitative predictions of polymer configurational statistics can be made from first principles using RIS theory.

CONCLUSIONS

Conformational energy calculations using the method of free optimization indicate that a three-state RIS model is appropriate for polystyrene. Rotation about bonds connecting the phenyl substituents to the polymer backbone lowers the energy of $\bar{g}$ states which were ignored in the original two-state scheme.

Even so, the two-state model (which was adjusted to match experiment) provides more accurate predictions of the characteristic ratio than the *ab initio* three-state model. The three-state model correctly predicts a higher limiting characteristic ratio for the syndiotactic polymer as compared to the isotactic, but the predicted values of C_∞ are rather low in both cases.

Molecular dynamics simulations on a periodic cell containing polystyrene fragments in a Θ solvent show that the solvent stabilization of *open* states is dominated by van der Waals interactions. The simulations allow an estimate of the magnitude of the short-range solvent effect

to be made, and, in the case of polystyrene, *open* states are found to be stabilized by about 1 kcal mol^{-1} relative to *closed* states. There are some quantitative differences compared to an alternative method of correcting for short-range solvent effects, which involves truncating the non-bond potential functions at a somewhat arbitrary distance[9], but corrections of the same order of magnitude result.

A perturbation method is used to correct the statistical weights of the three-state RIS model to account for short-range solvent stabilization of *open* states. This gives rise to opposite effects on the predicted characteristic ratios of isotactic and syndiotactic polystyrene, the former decreasing and the latter increasing. Thus the solvent effect is seen to enhance the tendency of the syndiotactic chain to expand relative to the isotactic chain. After solvent correction, C_∞ is predicted about 26–28% too low for both tacticities, a deviation attributable to errors arising from other approximations inherent in the RIS method. A 20% increase in the torsional force constants describing rotation about C–C bonds is found to alter the predicted characteristic ratios by a similar amount to the short-range solvent effect. This time C_∞ is increased for both the isotactic and syndiotactic chains.

The molecular dynamics simulations described above give a valuable insight into the effect of solvent interactions on the configurational statistics of polystyrene chains, and enable RIS models to be corrected for short-range solvent effects in a systematic manner.

ACKNOWLEDGEMENTS

Extremely helpful discussions with Dr Dana Honeycutt, Dr Omer Akgiray and Professor Lucien Monnerie are gratefully acknowledged.

REFERENCES

1 Flory, P. J. 'Statistical Mechanics of Chain Molecules', Interscience, New York, reprinted edition, 1989
2 'Polymer User Guide', version R-5.1, Biosym Technologies, San Diego, 1992
3 Young, R. J. and Lovell, P. A. 'Introduction to Polymers', Chapman and Hall, London, 2nd Edn., 1991
4 Wu, S. *J. Polym. Sci., Polym. Phys. Edn.* 1989, **27**, 723
5 Graessley, W. W. and Edwards, S. F. *Polymer* 1981, **22**, 1329
6 Flory, P. J. and Semylen, J. A. *J. Am. Chem. Soc.* 1966, **88**, 3209
7 Bedford, S. E., Yu, K. and Windle, A. H. *J. Chem. Soc., Faraday Trans.* 1992, **88**, 1765
8 Flory, P. J. and Suter, U. W. *Macromolecules* 1975, **8**, 765
9 Yoon, D. Y., Sundararajan, P. R. and Flory, P. J. *Macromolecules* 1975, **8**, 776
10 Berkert, U. and Allinger, N. L. 'Molecular Mechanics', American Chemical Society, Washington, DC, 1982
11 'Discover User Guide', version R-5.1, Biosym Technologies, San Diego, 1992
12 Krigbaum, W. R., Carpenter, D. K. and Newman, S. *J. Phys. Chem.* 1958, **62**, 1586
13 Kurata, M. and Stockmayer, W. H. *Fortshr. Hochpolym.-Forsch.* 1963, **3**, 196
14 Brandrup, J. and Immergut, E. H. (Eds.) 'Polymer Handbook', Wiley, New York, 1989
15 Bovey, F. A., Hood, F. P., Anderson, E. W. and Snyder, L. C. *J. Chem. Phys.* 1965, **42**, 3900; Johnson, L. F., Heatley, F. and Bovey, F. A. *Macromolecules* 1970, **3**, 175
16 Kuwahara, N., Saeki, S., Konno, S. and Kaneko, M. *Polymer* 1974, **15**, 66; Cotton, J. P., Decker, D., Benoit, H., Farnoux, B., Higgins, J., Jannik, G., Ober, R., Picot, C. and des Cloizeaux, J. *Macromolecules* 1974, **7**, 863
17 Allen, M. P. and Tildesley, D. J. 'Computer Simulation of Liquids', Clarendon, Oxford, 1987
18 Connolly, M. L. 'Molecular Surface Program', *Quantum Chem. Program. Exch. Bull.* 1981, **1**, 75

APPENDIX

Statistical weight matrices for bond pairs A, B and C from the free optimization calculations

The statistical weight is given by $A_{jk}\exp[-(\varepsilon_{jk}/RT)]$, and entries in *Tables 5–7* are in the form $\{A_{jk}, \varepsilon_{jk}\}$.

Table 5 Fragment A; bond angle supplement = 68.3°

	$\bar{g}$	t	g
$\bar{g}$	{1.29, 3.48}	{1.00, 0.35}	{1.15, 1.55}
t	{0.81, 0.90}	{1.00, 0.00}	{0.95, 1.04}
g	{0.91, 1.99}	{0.92, 0.73}	{1.17, 1.19}

Table 6 Fragment B; bond angle supplement = 68.7°

	$\bar{g}$	t	g
$\bar{g}$	{1.74, 3.61}	{1.12, 1.59}	{1.66, 2.88}
t	{1.45, 3.03}	{1.00, 0.00}	{1.58, 1.89}
g	{1.13, 2.94}	{1.29, 1.38}	{1.31, 2.12}

Table 7 Fragment C; bond angle supplement = 66.5°

	$\bar{g}$	t	g
$\bar{g}$	{1.29, 1.67}	{1.16, 0.18}	{1.2, 0.36}
t	{1.19, 1.16}	{1.00, 0.00}	{1.04, 0.18}
g	{1.28, 1.28}	{1.01, 0.17}	{1.01, 0.36}